ChemPubSoc Europe

DOI: 10.1002/slct.201701934

Chemistry SELECT Full Papers

Electro, Physical & Theoretical Chemistry

The Role of Partial Atomic Charge Assignment Methods on the Computational Screening of Metal-Organic Frameworks for CO_2 Capture under Humid Conditions

Wei Li,[a, b, c] Zizhen Rao,[a, b, c] Yongchul G. Chung,[d] and Song Li*[a, b, c]

Molecular simulations were carried out to compare the results from two different partial charge assignment strategies: extended charge equilibration (EQeq), and density derived electrostatic and chemical (DDEC), by computing the Henry's law constants of CO_2, H_2O, and N_2 for computation-ready, experimental (CoRE) MOFs. The Spearman's ranking correlation coefficient (SRCC) of the CO_2/H_2O selectivity rankings of MOFs with DDEC and EQeq charges based on the Henry's law constants showed that 8 out of the top 15 MOFs from screenings of MOFs with DDEC and EQeq charges were identical. We found that the most significant difference was observed in the adsorption energy for H_2O molecules, which showed large contribution from electrostatic interactions in H_2O adsorption energy, and for CO_2 and N_2 adsorption energies, van der Waals interaction energies played a major role.

Introduction

The greenhouse effect is intensified by the increasing anthropogenic CO_2 emissions mainly from combustion of fossil fuels. The continued development of efficient carbon capture technologies, including solvent absorption,[1] membrane separation[2] and solid adsorption[3] is the key to mitigate global climate change,[4] among which CO_2 adsorption by porous materials has attracted increasing research interests due to its low energy cost and facile operation.[1,2,5] In the recent decade, nanoporous metal-organic frameworks (MOFs) consisting of inorganic metal nodes and organic ligands have been one of the most promising adsorbents for carbon capture from flue gas because of their ultrahigh surface area, high thermal stability and structural tunability.[5,6] However, the presence of water vapor in the flue gas that competes the adsorption sites with CO_2 molecules in frameworks could adversely reduce the CO_2 adsorption capacity.[7,8] In addition, removal of water vapor from flue gas by decreasing the temperature could add up to the total cost of carbon capture.[9] Therefore, the design and discovery of MOFs that can preferentially adsorb CO_2 in the presence of water vapor is an important research area.[10]

Given that there are more than 6,000 MOFs reported in the literature[11] and hundreds of thousands of MOFs has been computationally generated so far,[11] high-throughput computational screening becomes an effective strategy to quickly identify the high-performing target MOFs from a huge number of existing and hypothetical structures[11,12] prior to performing extensive experimental studies of any specific MOF, which has been successfully employed for CO_2/N_2 and CO_2/CH_4 separations,[13] CH_4 storage,[11] H_2 storage,[14] Xe/Kr separation[15] and so on. Nevertheless, conventional high-throughput computational screenings based on grand canonical Monte Carlo (GCMC) simulations are computationally demanding tasks for modeling water adsorption. In order to reduce the computational efforts, high-throughput computational screening based on the Henry's law constants of adsorbate molecules that describe the adsorbate affinity towards frameworks in the limit of low pressure has been popularized in recent studies. Such a strategy has greatly accelerated the screening of MOFs for CO_2/H_2O,[10] NH_3/H_2O,[16] and hexane isomer separations.[17] Previously, we found that the partial charges of frameworks atoms are essential for accurately evaluating the affinity of H_2O molecules inside MOF frameworks at low pressure.[10] So far, EQeq method[18] has been frequently used to assign partial atomic charges to framework atoms to enable high-throughput computational screening of MOFs. Meanwhile, density functional theory (DFT) derived charge assignment strategies including ChelpG,[19] repeating electrostatic potential extracted atomic (REPEAT)[20] and density derived electrostatic and chemical (DDEC)[21] with high accuracy were also taken into account for more accurately describing electrostatic potential of MOF frameworks. However, due to the high computational cost, DFT derived charge assignments were rarely used for high-throughput computational screening. Besides expensive

[a] W. Li, Z. Rao, Prof. S. Li
State Key Laboratory of Coal Combustion, School of Energy and Power Engineering, Huazhong University of Science and Technology, 1037 Luoyu Road, Wuhan, 430074, China
E-mail: songli@hust.edu.cn
[b] W. Li, Z. Rao, Prof. S. Li
Shenzhen Research Institute of Huazhong University of Science and Technology, Shenzhen, 518057, China.
[c] W. Li, Z. Rao, Prof. S. Li
Nano Interface Centre for Energy, School of Energy and Power Engineering, Huazhong University of Science and Technology, 430074, China.
[d] Prof. Y. G. Chung
School of Chemical and Biomolecular Engineering, Pusan National University, 46421, Busan, Korea (South).

Supporting information for this article is available on the WWW under https://doi.org/10.1002/slct.201701934

computation, the employment of the cluster structure for calculating electrostatic potential of periodic frameworks is another drawback of ChelpG method, which ignores the atomic coordination environments, and may cause the chemically unrealistic partial atomic charge for MOFs. REPEAT[20] method was developed to obtain the partial charges of periodic structures by fitting the electrostatic potential, but it has limited applicability to porous structures, especially for structures with buried atoms. DDEC[21] was assumed to provide the most realistic partial charges for periodic MOF frameworks since both chemical environment and meaningfulness were taken into consideration. Nevertheless, DDEC method was rarely applied in high-throughput computational screening due to its high computational cost for obtaining the electrostatic potential from DFT calculations for a large number of frameworks. Recently, Nazarian and co-workers[22] have successfully assigned DDEC charges to 2932 CoRE MOF structures,[12] and screened the MOFs with DDECs charges for tert-butyl mercaptan/CH_4 separations. CoRE MOF DDEC database opens up an opportunity to computationally screen MOFs for CO_2/H_2O separation, and to compare two different partial charge assignment methods.

Our previous study[10] on computational screening of CoRE MOFs with EQeq charges for CO_2/H_2O separation has shown that H_2O adsorption in MOF frameworks is dominated by electrostatic interactions, suggesting the importance of using an accurate partial atomic charge assignment method in evaluating the affinity of H_2O molecules in MOF structures based on Henry's law constant calculations. However, the effectiveness of this partial atomic charge assignment method for CoRE MOF database compared with more accurate DDEC charges has not been investigated so far. In this work, CoRE MOF frameworks carrying EQeq and DDEC partial atomic charges were computationally screened using the Henry's law constant calculations to discover high selective MOFs toward CO_2 in the presence of H_2O molecules. Following the screening, we compared the top 15 MOFs from EQeq and DDEC CoRE MOF database to investigate the discrepancy originated from different partial atomic charge assignment strategies, and analyzed the adsorption energy and isotherms of selected MOFs to understand the observed tendency.

Results and Discussion

The schematic illustration of screening procedure is presented in Scheme 1. All MOF structures were obtained from the computation-ready, experimental (CoRE) MOF database Version 1.0,[12] which is the largest experimentally synthesized MOF database. The structures of CoRE MOF DDEC database were obtained from Nazarian and co-workers,[22] which contains 2932 experimentally CoRE MOF structures. After removing the structures with zero accessible surface area (ASA) and non-MOF structures, the rest of 1627 MOFs with DDEC and EQeq[18] charges, respectively were used to calculate Henry's law constants of CO_2, H_2O and N_2. The CO_2/H_2O selectivity of MOFs based on Henry's law constants was defined as the Henry's law constants ratio of CO_2 and H_2O in Equation 1:

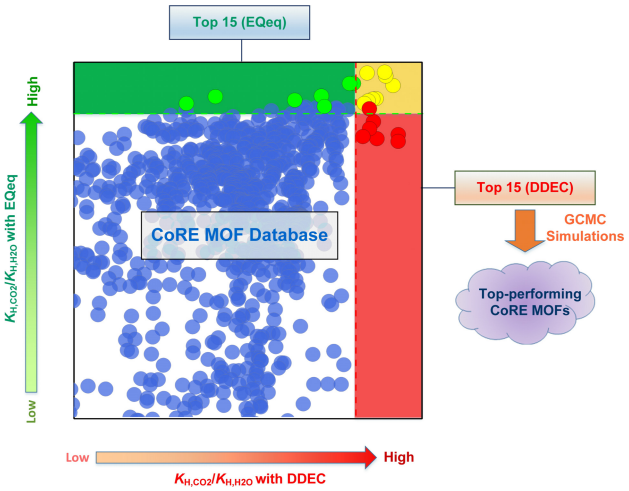

Scheme 1. Schematic illustration of screening procedure

$$S_{KH} = \frac{K_{H,CO2}}{K_{H,H2O}} \quad (1)$$

Due to the limited computational resources, the top 15 MOFs with DDEC and EQeq charges were selected for further GCMC simulations, respectively, according to the ranking of their CO_2/H_2O selectivity from Henry's law constants (S_{KH}), which were supposed to exhibit high selective adsorption towards CO_2 in the presence of water vapor.

The CO_2/H_2O selectivity(S_{KH}) from Henry's law constants of 1627 MOFs with DDEC and EQeq charges were plotted as a function of largest cavity diameter(LCD) as shown in Figure 1. We found that MOFs structures with high CO_2/H_2O selectivity exhibited extremely small pore size (~5 Å), relatively low surface area ($<1000\ m^2/g$) and low void fraction (<0.6) regardless of the atomic charge assignment methods for MOF frameworks.

Further analysis was performed to compare the effects of DDEC and EQeq charges of MOFs on Henry's law constants of each adsorbate (Figure 2). First of all, there are obvious differences observed for the Henry's law constants(K_H) of CO_2, H_2O and N_2 within MOFs carrying DDEC and EQeq charges (Figure 2a), respectively. For a majority of MOF structures, their Henry's law constants of CO_2 are similar regardless of the partial atomic charge assignment methods (DDEC or EQeq). We also found that only a few structures exhibited low $K_{H,CO2}$ (DDEC) compared with $K_{H,CO2}$(EQeq), suggesting that EQeq generally overestimates $K_{H,CO2}$ compared with DDEC. We also observed deviations between the Henry's law constants of H_2O for the MOFs with DDEC charges and those with EQeq charges. 264 MOFs with DDEC charges showed much higher $K_{H,H2O}$(DDEC) in contrast to $K_{H,H2O}$(EQeq) with $K_{H,H2O}$(DDEC) / $K_{H,H2O}$(EQeq) $>1{,}000$, but we found that 14 MOFs showed extremely high $K_{H,H2O}$ (EQeq) ($>1\times10^{29}$ mol/kg•Pa) in comparison with $K_{H,H2O}$(DDEC) with a large deviation of $K_{H,H2O}$(DDEC)/ $K_{H,H2O}$(EQeq) $<1\times10^{-30}$, which can be attributed to the discrepancy in partial atomic charges of the MOFs predicted by DDEC and EQeq, as shown in Table S1 of Supporting Information(SI).

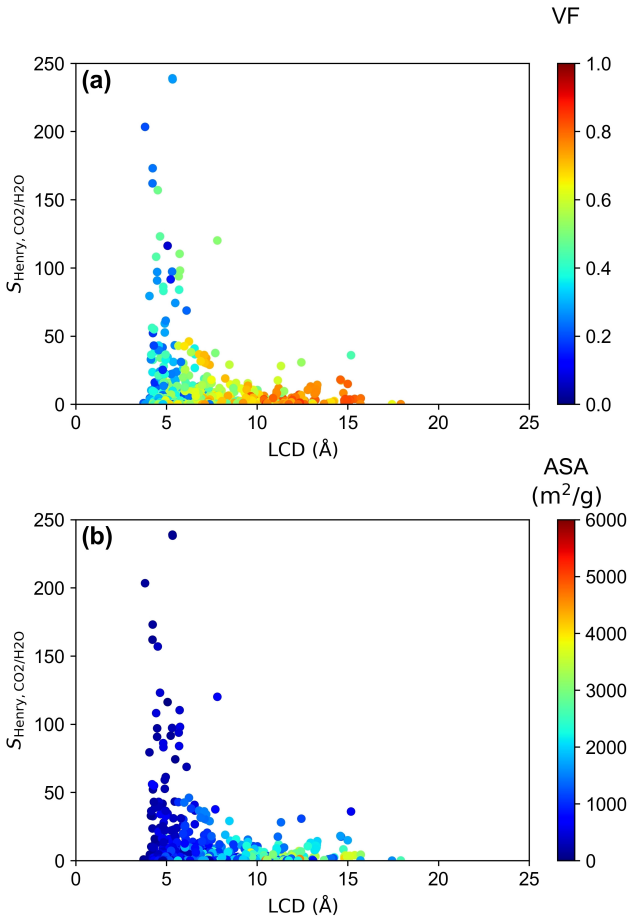

Figure 1. CO_2/H_2O selectivity based on the ratio of Henry's constants against the largest cavity diameter (LCD) for 1627 CoRE MOF structutres using DDEC charges. Data points are colored based on (a) the accessible surface area (ASA) and (b) the void fraction (VF), respectively.

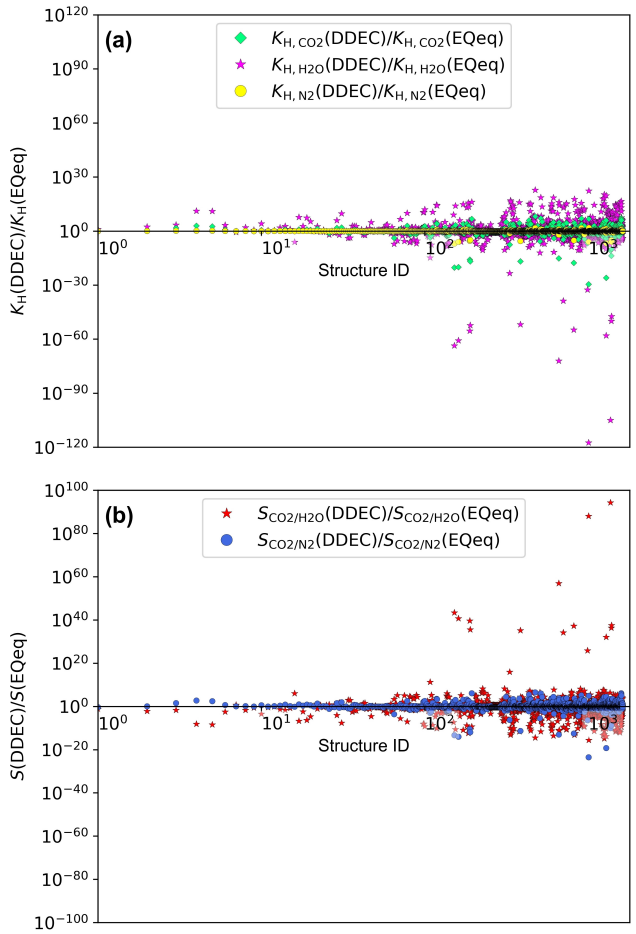

Figure 2. Comparison of the calculated Henry's law constant (K_H) and selectivity(S_{KH}) for 1627 CoRE MOFs with DDEC and EQeq charges, respectively. (a) The ratio of Henry's law constants (K_H) of CO_2, H_2O and N_2 for MOFs with DDEC charges to those with EQeq charges;(b) The ratio of S_{KH} of CO_2/H_2O and CO_2/N_2 for MOFs with DDEC charges to those with EQeq charges.

However, the Henry's law constants of N_2 for MOFs was least influenced by the methods of charge assignments, which displayed nearly identical $K_{H,N2}$(DDEC) and $K_{H,N2}$(EQeq) for all MOFs. The results indicate that the Henry's law constants are sensitive to the polarity of adsorbates: e.g., H_2O molecule has a dipole moment of 1.84 D, whereas CO_2 and N_2 exhibit zero dipole moment, but the quadrupole moments of CO_2 is larger than N_2. On the basis of this, the partial atomic charge assignment methods affect the Henry's law constants of H_2O the most, followed by CO_2 and N_2. Similarly, when comparing the selectivity (S_{KH}) of CO_2/H_2O and CO_2/N_2, a pronounced deviation was observed between $S_{KH,CO2/H2O}$ of MOFs with DDEC and those with EQeq charges. Due to the extremely low $K_{H,H2O}$ of 14 MOFs with DDEC charges shown in Table S1, their $S_{KH,CO2/H2O}$ from DDEC is higher than 1×10^{25} times of those with EQeq charges. The Spearman's ranking correlation coefficient (SRCC) ranging from -1 to $+1$ that describes the correlation between two sets of ranking lists, is 0.53 comparing the CO_2/H_2O selectivity($S_{KH,CO2/H2O}$) ranking of MOFs with DDEC charges and those with EQeq charges. The analysis suggests that the screening results based on the MOFs with DDEC charges are positively correlated with those with EQeq charges, and the strength of their correlation is moderate (~0.53). On the contrary, the SRCC of CO_2/N_2 selectivity ranking between MOFs with DDEC and EQeq charges is slightly smaller (~0.49), indicating the relatively weak correlation.

From the screening, the top 15 MOFs with highest $S_{KH,CO2/H2O}$ (DDEC) and $S_{KH,CO2/H2O}$ (EQeq) were selected as shown in Table 1 and 2, respectively. 8 out of the 15 structures from Table 1 can be found in Table 2, suggesting that the computational screening using EQeq charges is effective for the system that we investigated. We also noticed that the 15 selected MOFs exhibited low surface area (<1000 m^2/g) and small pore size (~5 Å). Moreover, it should be noted that among the selected top MOFs, PUQYAC and PUQXUV are a pair of enantiomers, both of which exhibited hydrophobic channels[23] with high CO_2/H_2O selectivity as predicted by our calculation in this work. In addition, the experimental measurement by Comotti *et al.*[28] revealed that WOJJOV exhibited evidently high CO_2 adsorption but no H_2O uptake until approximately $P/P_0=0.4$, suggesting

Table 1. The top 15 structures with DDEC charges from screening based on the ratio of Henry's law constants between CO_2 and H_2O

REFCODE	VF	ASA (m^2/g)	LCD (Å)	$S_{KH\text{-}DDEC}$	$S_{KH\text{-}EQeq}$	$S_{MC\text{-}DDEC}$	ΔN_{DDEC} (mol/kg)	$S_{MC\text{-}EQeq}$	ΔN_{EQeq} (mol/kg)
PUQYAC[23]	0.28	114	5.33	239	56	113	0.51	7	0.50
PUQXUV[23]	0.28	124	5.34	238	45	112	0.51	4	0.50
PAPXUB[24]	0.20	147	3.82	203	247	97	0.77	119	0.80
KAXQOR[25]	0.23	139	4.23	162	328	50	0.60	102	0.67
PARMIG[26]	0.48	364	4.52	157	370	31	1.36	88	1.32
PAVLUU[27]	0.46	466	4.65	123	49	38	2.10	24	1.53
WOJJOV[28]	0.51	638	7.81	120	166	27	1.21	0.59	1.30
BUSQEM[29]	0.51	439	5.73	110	82	42	2.01	22	2.09
VICDOC[30]	0.45	503	4.43	108	163	37	2.03	88	1.85
MUVGUG[31]	0.51	546	5.75	98	67	22	2.00	18	2.21
PIHJOH[32]	0.24	303	5.31	97	122	50	0.70	73	0.68
MUVHER[31]	0.52	431	5.68	94	155	30	2.02	52	2.09
LIDZUV[33]	0.27	186	4.49	91	360	5	0.58	110	0.59
PEYSIW[34]	0.40	563	5.70	84	133	30	1.72	67	1.64
DEGJIK[35]	0.28	207	4.07	79	52	56	1.23	28	1.28

GCMC simulations of $CO_2/H_2O/N_2$ mixture with a molar ratio of 9672:3280:87048 were performed at 298 K for MOFs carrying DDEC or EQeq charges. The CO_2/H_2O selectivity ($S_{MC\text{-}DDEC}$ and $S_{MC\text{-}DDEC}$) was calculated according to Eq. S2 in Supporting Information(SI) from GCMC simulation of ternary mixture at 1 bar. The CO_2 working capacity (ΔN_{DDEC} and ΔN_{EQeq}) was obtained by subtracting the CO_2 adsorption capacity of MOFs at 0.1 bar from the adsorption capacity at 1 bar from GCMC simulation of $CO_2/H_2O/N_2$ mixture as described in Eq. S3.

Table 2. The top 15 MOFs with EQeq charges from screening based on the ration of Henry's law constant between CO_2 and H_2O

REFCODE	VF	ASA (m^2/g)	LCD (Å)	$S_{KH\text{-}DDEC}$	$S_{KH\text{-}EQeq}$	$S_{MC\text{-}DDEC}$	ΔN_{DDEC} (mol/kg)	$S_{MC\text{-}EQeq}$	ΔN_{EQeq} (mol/kg)
PARMIG[26]	0.48	364	4.52	157	370	31	1.36	87	1.32
LIDZUV[33]	0.27	186	4.49	91	360	5	0.58	110	0.59
KAXQOR[25]	0.23	139	4.23	162	328	39	0.60	102	0.67
LEZZEX[33]	0.29	250	4.91	59	263	2	0.63	80	0.66
LIDZOP[33]	0.29	248	4.91	53	262	3	0.65	64	0.66
PAPXUB[24]	0.20	147	3.82	203	247	97	0.77	119	0.80
MIMVEJ[36]	0.47	439	4.57	22	179	0.21	0.90	73	1.60
IWELOM[37]	0.37	228	4.71	0.81	176	0.04	0.39	61	1.01
WOJJOV[28]	0.51	638	7.81	120	166	27	1.21	0.59	1.30
VICDOC[30]	0.45	504	4.43	108	163	36	2.03	88	1.85
EMIVAY[38]	0.39	378	5.17	9.6	158	0.03	-0.21	34	1.70
MUVHER[31]	0.52	431	5.68	94	155	30	2.02	52	2.09
PEYSIW[34]	0.40	563	5.70	84	133	30	1.72	67	1.64
IWELIG01[39]	0.37	202	4.59	0.33	143	0.05	0.39	59	1.01
PEPKUR[40]	0.29	192	4.64	24	130	9	0.95	67	0.97

GCMC simulations of $CO_2/H_2O/N_2$ mixture with a molar ratio of 9672:3280:87048 were performed at 298 K for MOFs carrying DDEC or EQeq charges. The CO_2/H_2O selectivity ($S_{MC\text{-}DDEC}$ and $S_{MC\text{-}DDEC}$) was calculated according to Eq. S2. from GCMC simulation of ternary mixture at 1 bar. The CO_2 working capacity (ΔN_{DDEC} and ΔN_{EQeq}) was obtained by subtracting the CO_2 adsorption capacity of MOFs at 0.1 bar from the adsorption capacity at 1 bar from GCMC simulation of $CO_2/H_2O/N_2$ mixture as described in Eq. S3.

the high affinity of WOJJOV towards CO_2 than H_2O molecules, consistent with our prediction.

For the 15 MOFs in Table 1, we calculated the CO_2/H_2O selectivity based on Henry's law constant using both DDEC($S_{KH\text{-}DDEC}$) and EQeq charges($S_{KH\text{-}EQeq}$). Comparing $S_{KH\text{-}DDEC}$ and $S_{KH\text{-}EQeq}$, both $S_{KH\text{-}DDEC}$ and $S_{KH\text{-}EQeq}$ are in the same order of magnitude and they are greater than 1 (shown in Table 1), implicating the favorable adsorption of CO_2 over H_2O for the selected structures from MOFs with DDEC charges. Nevertheless, for the top 15 MOFs selected from the MOFs with EQeq charges (Table 2), their CO_2/H_2O selectivity($S_{KH\text{-}EQeq}$) is generally over-estimated by EQeq charge in contrast with $S_{KH\text{-}DDEC}$, and their discrepancy is up to three orders of magnitude. Additionally, 2 out of 15 MOFs, e.g., IWELOM and IWELIG01, which is a pair of enantiomers, have $S_{KH\text{-}DDEC} < 1$, suggesting 13% of 15 selected structures from the MOFs with EQeq charges exhibits the favorable adsorption of H_2O rather than CO_2 molecules. In brief, the top-performing MOFs selected from MOFs with DDEC charges exhibit high CO_2/H_2O selectivity regardless of the methods of partial atomic charge assignment. The CO_2/H_2O selectivity (S_{MC}) of selected MOFs with DDEC and EQeq charges obtained from GCMC simulations of $CO_2/H_2O/N_2$ ternary mixture was generally smaller compared with the selectivity (S_{KH}) from Henry's law constants, but similar tendency in $S_{MC\text{-}DDEC}$ and. $S_{MC\text{-}EQeq}$ was observed comparing with $S_{KH\text{-}DDEC}$ and $S_{KH\text{-}EQeq}$.

The selected MOFs with DDEC partial atomic charges (Table 1) obtained from GCMC simulations exhibited similar CO_2 working capacity to those with EQeq charges. On the contrary,

most of the selected MOFs with EQeq charges(Table 2) shown larger CO_2 working capacity than those with DDEC charges, and the pronounced deviation was observed for MIMVEJ, IWELOM, EMIVAY and IWELIG01 that preferentially adsorbed H_2O instead of CO_2 with CO_2/H_2O selectivity of $S_{MC\text{-}DDEC} < 1$, which is correlated with the deviation in their atomic partial charges of MIMVEJ, IWELOM, EMIVAY and IWELIG01 obtained from DDEC and EQeq methods shown in Table S2.

The location of the selected top performers in the plot of Henry's law constants of MOF database with DDEC versus those with EQeq charges was shown in Figure 3. The Henry's law constants of CO_2 for most of the selected MOFs were located on the red line (Figure 3a), indicating the nearly identical Henry's law constant of CO_2 for MOFs with DDEC and EQeq charges. Whereas, the deviation was observed in Henry's law constant of H_2O (Figure 3b) for MOFs from EQeq-based screening (in green), whose selectivities ($K_{H,H2O}$) were evidently underestimated by EQeq charges in contrast to the results from DDEC. Thus the CO_2/H_2O selectivity of MOFs (in green) from EQeq-based screening apparently drifted away from the red line and was overestimated by EQeq charges compared with DDEC (Figure 4a).

Nevertheless, Henry's law constants of N_2 for all the selected MOFs from both screenings based on DDEC or EQeq charges were identical, leading to similar CO_2/N_2 selectivity of selected MOFs (in green) in Figure 4b. Such tendencies were correlated with the polarity of adsorbates, similar to the observations in Figure 2, which was also supported by the adsorption energy of each type of adsorbates within selected MOFs with DDEC charges as shown in Figure 5. In addition, there is only slight difference observed in CO_2 adsorption energy (Figure 5) of selected MOFs with DDEC charges and EQeq charges, and van der Waals interaction played a dominant role in CO_2 adsorption. The nearly identical N_2 adsorption energy (Figure 5c) was found for MOFs with DDEC and EQeq charges, respectively, which was also dominated by van der Waals interaction.

H_2O adsorption energy (Figure 5b) of the selected MOFs with DDEC and EQeq charges, respectively, exhibit significant difference compared with CO_2 (Figure 5a) and N_2 adsorption energy (Figure 5c), suggesting the high sensitivity of the H_2O molecules to atomic partial charges as reported in previous study,[10] and the electrostatic interactions were dominant for H_2O adsorption inside MOFs with either DDEC or EQeq charges. The total CO_2 adsorption energy is highest followed by H_2O and N_2, which was observed in selected MOFs with DDEC and EQeq charges, respectively. Similar tendency was observed for the top 15 candidates (Table 2) from screening of MOFs with EQeq charges as shown in Figure S1 of SI.

Besides CO_2/H_2O selectivity, CO_2 adsorption capacity is another important criterion to evaluate CO_2/H_2O separation performance. To assess the CO_2 adsorption capacity of highly selective MOFs, 6 MOFs with the highest CO_2/H_2O selectivity based on Henry's law constant or CO_2 working capacity were chosen from Table 1 for further detailed GCMC simulations. Among the 6 structures, PUQYAC and PUQXUV exhibited the highest CO_2/H_2O selectivity of 113 and 112, respectively, and PAVLUU, BUSQEM, VICDOC and MUVHER have the highest CO_2

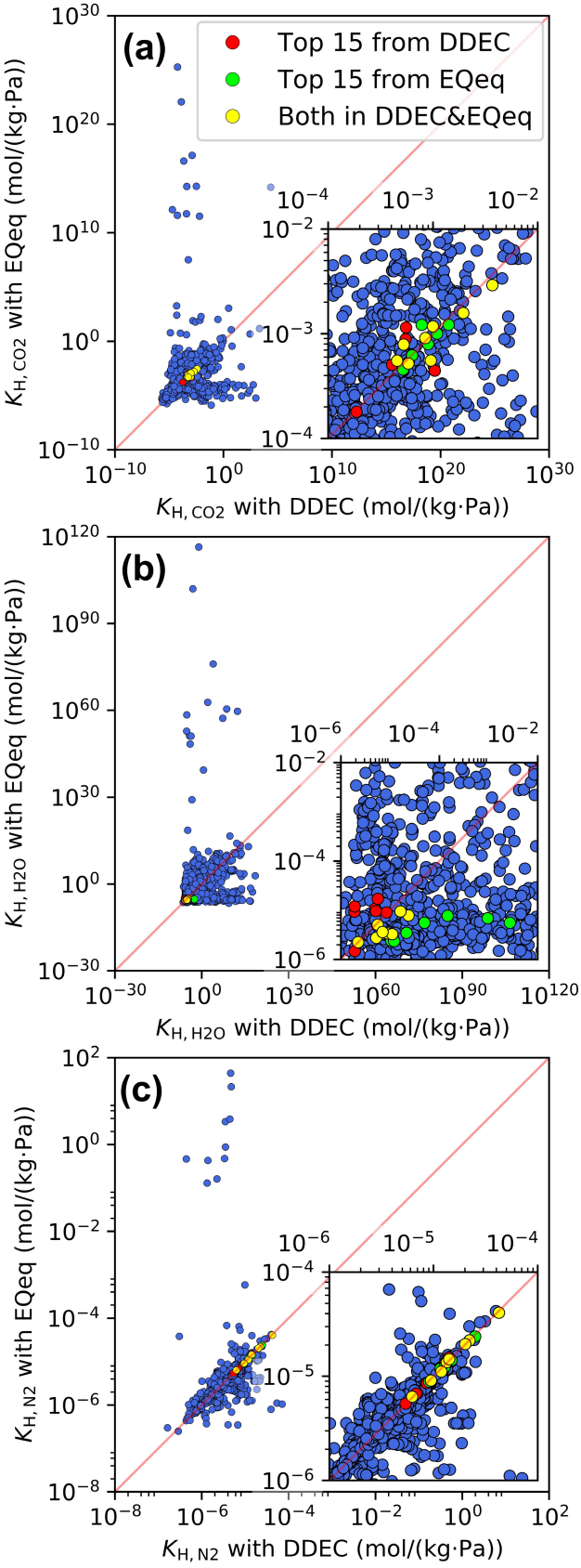

Figure 3. Henry's law constants (K_H) of (a) CO_2, (b) H_2O and (c) N_2 of 1627 MOF strcutures with DDEC charges versus those with EQeq charges, respectively.

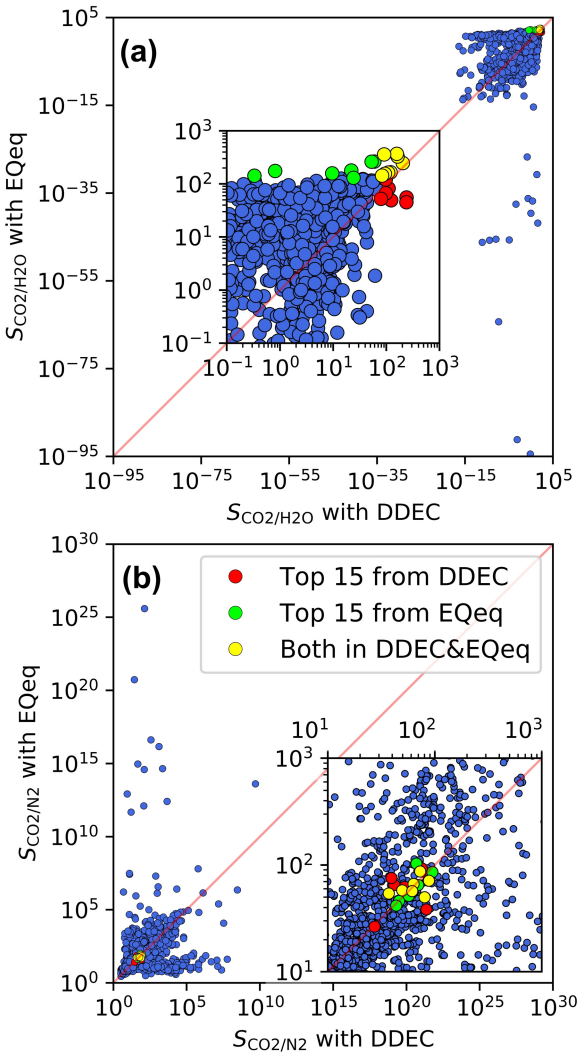

Figure 4. The Henry's selectivity (S_{KH}) of (a) CO_2/H_2O and (b) CO_2/N_2 based on the ratio of Henry's constants of CO_2, H_2O and N_2 of MOFs with DDEC charges versus those with EQeq charges. The selected top 15 MOFs with DDEC (in red and yellow) and EQeq (in green and yellow) charges were highlighted,respectively.

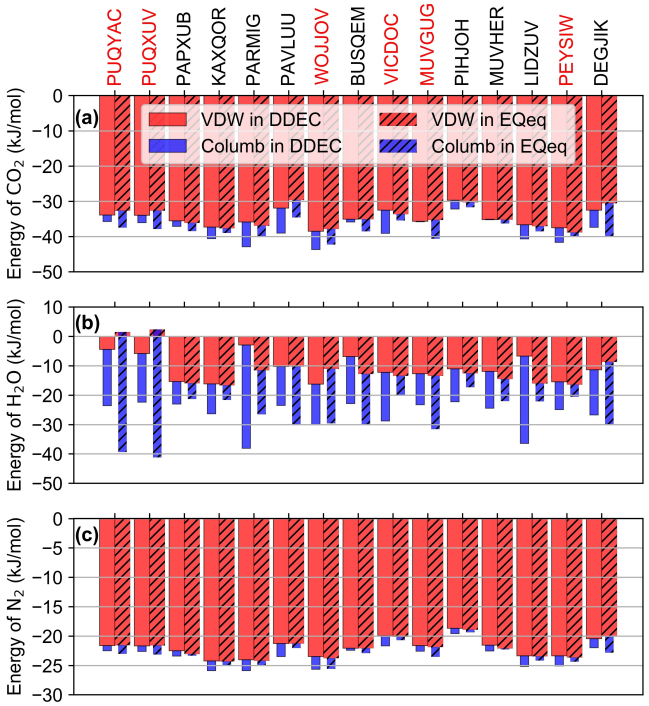

Figure 5. Adsorption energy of (a) CO_2, (b) H_2O and (c) N_2 within selected MOFs from DDEC-based screening(as shown in Table 1), respectively. The REFCODE in red is the top 6 MOFs with high CO_2/H_2O selectivity according to GCMC simulation of $CO_2/H_2O/N_2$ mixture at 1 bar.

adsorption working capacity of above 2 mol/kg. Their adsorption isotherms from GCMC simulation of $CO_2/H_2O/N_2$ ternary mixture ranging from 0.05 to 1 bar were shown in Figure 6, in which all the 6 MOFs exhibited high CO_2 adsorption, low N_2 adsorption and no water adsorption. It should be noted that PUQYAC[23] and PUQXUV[23] exhibited similar CO_2 working capacity of 0.51 mol/kg. On the contrary, PAVLUU, BUSQEM, VICDOC and MUVHER exhibit much higher CO_2 working capacity of 2.10, 2.01, 2.03 and 2.02 mol/kg with the CO_2/H_2O selectivity of 38, 42, 37 and 30. The suitable adsorbent for CO_2/H_2O separation should have both high selectivity and adsorption capacity. In this aspect, PAVLUU, BUSQEM, VICDOC and MUVHER are better choices for CO_2 capture in the presence of water vapor. According to the snapshots shown in Figure 7, the major pore space of selected MOFs were filled with CO_2 molecules, all of which were located in the center of pores, whereas, little H_2O and N_2 molecules were found, which is consistent with the high CO_2/H_2O selectivity based on Henry's law constants calculation in Table 1.

Conclusions

This work investigated the impact of the atomic charge assignment strategies of MOFs, i.e. DDEC and EQeq charges, on high-throughput computational screening for CO_2/H_2O separation. We found that similar Henry's law constants of CO_2 and N_2 were obtained for MOFs with DDEC and EQeq partial atomic charges, whereas, the significant deviation in Henry's law constants of H_2O was observed, which leads to the underestimation of CO_2/H_2O Henry selectivity by EQeq partial atomic charges compared to DDEC charges. The moderate correlation was also observed in SRCC of the ranking of CO_2/H_2O selectivity of CoRE MOFs with DDEC and EQeq charges. Moreover, 8 out of 15 top-performing MOFs discovered from screenings of MOFs with DDEC and EQeq charges suggested the relatively moderate reliability of EQeq charge assignment for CoRE MOF screening. However, given that only the top 15 performers were adopted for analysis, the conclusion drawn above may be modified if more top performers were taken into account. In addition, the dominant role of van der Waals interactions in the adsorption of CO_2 and N_2, and the importance of electrostatic interactions for H_2O adsorption for selected MOFs with high CO_2/H_2O selectivity was found in MOFs regardless of the partial

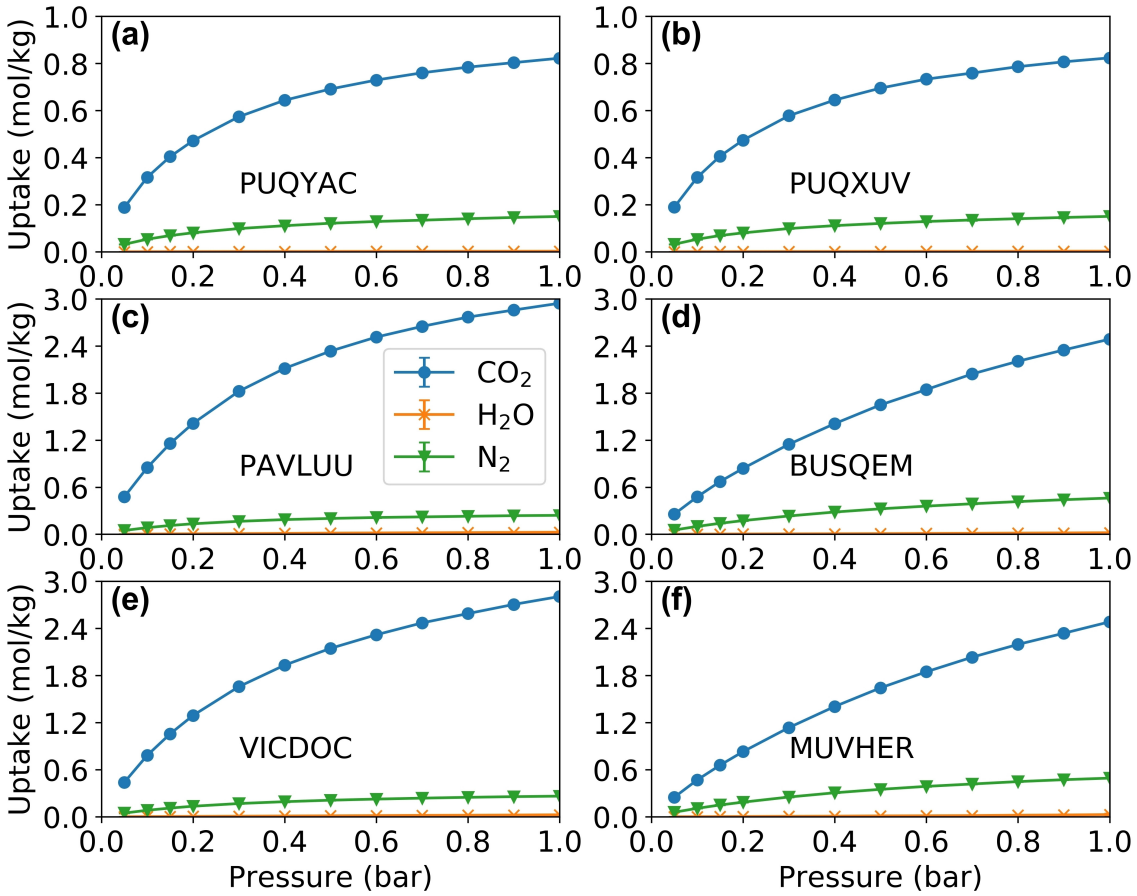

Figure 6. CO_2, H_2O and N_2 adsorption isotherms of top-performing MOFs for a ternary mixture of $CO_2/H_2O/N_2$ from GCMC simulation at 298 K (the molar ratio of $CO_2/N_2/H_2O$ is 9672/3280/87048). The error bars presented in the plot are too small to be discerned.

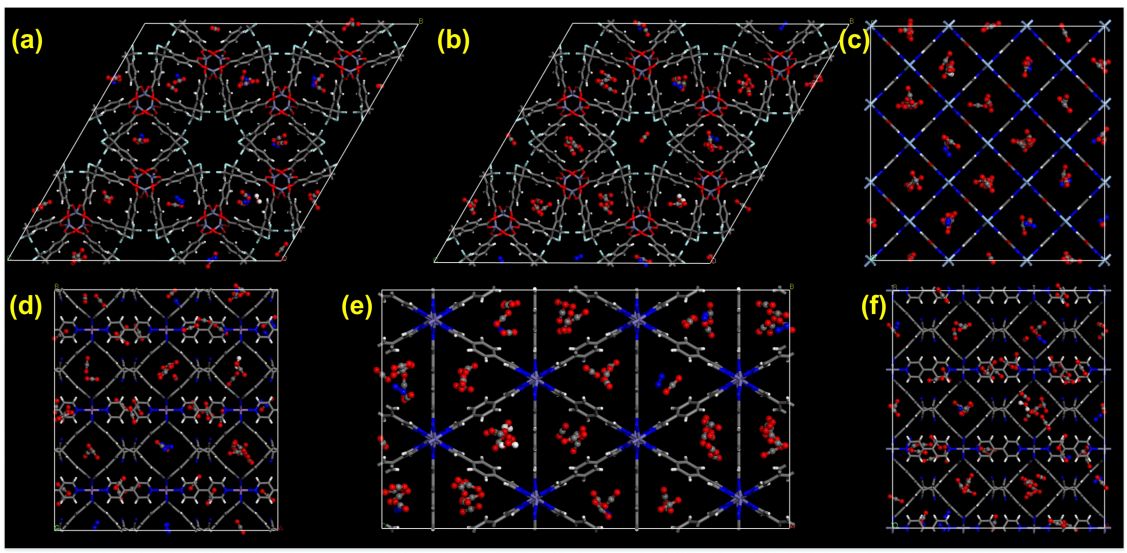

Figure 7. Snapshots from GCMC simulations of ternary mixture ($CO_2/H_2O/N_2$) at 298 K and 1 bar (a for PUQYAC, b for PUQXUV, c for PAVLUU, d for BUSQEM, e for VICDOC and f for MUVHER.

atomic charge assignment methods. The findings in this work will be of great interest for researchers in the MOF modeling

community, which provides fundamental understanding and molecular insights for accurately simulating water adsorption in MOFs by choosing suitable charge assignment strategies.

Supporting Information Summary

All computational details were provided in Supporting Information. Besides, the averaged atomic partial charges for selected MOFs, the Spearman's ranking correlation coefficients of CO_2, H_2O and N_2 between DDEC and EQeq, the force field parameters of the adsorbates, and the CO_2, H_2O and N_2 adsorption energy of MOFs selected from screening by EQeq charges were also presented in Supporting Information.

Acknowledgements

This work was supported by the National Natural Science Foundation of China under Grant No. 51606081 and Basic Research Foundation of Shenzhen under Project No. JCYJ20160506170043770. This work was carried out at the National Supercomputer Center in Tianjin, and the calculations were performed on TianHe-1 (A), and was supported by PLSI supercomputing resources of Korea Institute of Science and Technology Information (account: pe0673). Y.G.C. was supported by Basic Science Research Program through the National Research Foundation of Korea (NRF) funded by the Ministry of Education (NRF-2016R1D1 A1B03934484).

Conflict of Interest

The authors declare no conflict of interest.

Keywords: adsorption · atomic charges · interaction energy · selectivity

[1] H. Yang, Z. Xu, M. Fan, R. Gupta, R. B. Slimane, A. E. Bland, I. Wright *J. Environ. Sci.* **2008**, *20*, 14–27.
[2] D. M. D'Alessandro, B. Smit, J. R. Long *Angew. Chem.* **2010**, *122*, 6194–6219.
[3] S. Choi, J. H. Drese, C. W. Jones *ChemSusChem.* **2009**, *2*, 796–854.
[4] D. Y. C. Leung, G. Caramanna, M. M. Maroto-Valer *Renew. Sust. Energ. Rev.* **2014**, *39*, 426–443.
[5] J. Liu, P. K. Thallapally, B. P. McGrail, D. R. Brown, J. Liu *Chem. Soc. Rev.* **2012**, *41*, 2308–2322.
[6] K. Sumida, D. L. Rogow, J. A. Mason, T. M. McDonald, E. D. Bloch, Z. R. Herm, T.-H. Bae, J. R. Long *Chem. Rev.* **2012**, *112*, 724–781.
[7] A. C. Kizzie, A. G. Wong-Foy, A. J. Matzger *Langmuir.* **2011**, *27*, 6368–6373.
[8] J. Liu, A. I. Benin, A. M. B. Furtado, P. Jakubczak, R. R. Willis, M. D. LeVan *Langmuir.* **2011**, *27*, 11451–11456.
[9] K. T. Leperi, R. Q. Snurr, F. You *Ind. Eng. Chem. Res.* **2016**, *55*, 3338–3350.
[10] S. Li, Y. G. Chung, R. Q. Snurr *Langmuir.* **2016**, *32*, 10368–10376.
[11] C. E. Wilmer, M. Leaf, C. Y. Lee, O. K. Farha, B. G. Hauser, J. T. Hupp, R. Q. Snurr *Nat. Chem.* **2012**, *4*, 83–89.
[12] Y. G. Chung, J. Camp, M. Haranczyk, B. J. Sikora, W. Bury, V. Krungleviciute, T. Yildirim, O. K. Farha, D. S. Sholl, R. Q. Snurr *Chem. Mater.* **2014**, *26*, 6185–6192.
[13] C. E. Wilmer, O. K. Farha, Y. S. Bae, J. T. Hupp, R. Q. Snurr *Energ. Environ. Sci.* **2012**, *5*, 9849–9856.
[14] J. Goldsmith, A. G. Wong-Foy, M. J. Cafarella, D. J. Siegel *Chem. Mater.* **2013**, *25*, 3373–3382.
[15] D. Banerjee, C. M. Simon, A. M. Plonka, R. K. Motkuri, J. Liu, X. Y. Chen, B. Smit, J. B. Parise, M. Haranczyk, P. K. Thallapally *Nat. Commun.* **2016**, *7*, 11831.
[16] P. Z. Moghadam, D. Fairen-Jimenez, R. Q. Snurr *J. Mater. Chem. A.* **2016**, *4*, 529–536.
[17] Y. G. Chung, P. Bai, M. Haranczyk, K. T. Leperi, P. Li, H. Zhang, T. C. Wang, T. Duerinck, F. You, J. T. Hupp, O. K. Farha, J. I. Siepmann, R. Q. Snurr *Chem. Mater.* **2017**, *29*, 6318-6325.
[18] C. E. Wilmer, K. C. Kim, R. Q. Snurr *J. Phys. Chem. Lett.* **2012**, *3*, 2506–2511.
[19] C. M. Breneman, K. B. Wiberg *J. Comput. Chem.* **1990**, *11*, 361–373.
[20] C. Campana, B. Mussard, T. K. Woo *J. Chem. Theory Comput.* **2009**, *5*, 2866–2878.
[21] T. A. Manz, D. S. Sholl *J. Chem. Theory Comput.* **2010**, *6*, 2455–2468.
[22] D. Nazarian, J. S. Camp, D. S. Sholl *Chem. Mater.* **2016**, *28*, 785–793.
[23] H.-L. Jiang, B. Liu, Q. Xu *Cryst. Growth Des.* **2010**, *10*, 806–811.
[24] J. Xiao, C. X. Chen, Q. K. Liu, J. P. Ma, Y. B. Dong *Cryst. Growth Des.* **2011**, *11*, 5696–5701.
[25] D. Banerjee, Z. J. Zhang, A. M. Plonka, J. Li, J. B. Parise *Cryst. Growth Des.* **2012**, *12*, 2162–2165.
[26] L. Wu, M. Xue, L. Huang, S. L. Qiu *Sci. China Chem.* **2011**, *54*, 1441–1445.
[27] M. Du, X. J. Zhao, J. H. Guo, S. R. Batten *Chem. Commun.* **2005**, 4836–4838.
[28] A. Comotti, S. Bracco, P. Sozzani, S. Horike, R. Matsuda, J. Chen, M. Takata, Y. Kubota, S. Kitagawa *J. Am. Chem. Soc.* **2008**, *130*, 13664–13672.
[29] S. Shimomura, R. Matsuda, S. Kitagawa *Chem. Mater.* **2010**, *22*, 4129–4131.
[30] Z. R. Herm, B. M. Wiers, J. A. Mason, J. M. van Baten, M. R. Hudson, P. Zajdel, C. M. Brown, N. Masciocchi, R. Krishna, J. R. Long *Science.* **2013**, *340*, 960–964.
[31] S. Shimomura, M. Higuchi, R. Matsuda, K. Yoneda, Y. Hijikata, Y. Kubota, Y. Mita, J. Kim, M. Takata, S. Kitagawa *Nat. Chem.* **2010**, *2*, 633–637.
[32] G. B. Wang *Synth. React. Inorg. M.* **2013**, *43*, 1311–1314.
[33] C. T. Yeh, W. C. Lin, S. H. Lo, C. C. Kao, C. H. Lin, C. C. Yang *CrystEngComm.* **2012**, *14*, 1219–1222.
[34] T. K. Maji, R. Matsuda, S. Kitagawa *Nat. Mater.* **2007**, *6*, 142–148.
[35] K. Darling, W. Ouellette, J. Zubieta *Inorg. Chim. Acta.* **2012**, *392*, 52–60.
[36] B. Rather, B. Moulton, R. D. Bailey Walsh, M. J. Zaworotko *Chem. Commun.* **2002**, *7*, 694–695.
[37] X. H. Zhang, Z. M. Hao, X. M. Zhang *Chem-Eur J.* **2011**, *17*, 5588–5594.
[38] S. Xiong, S. Wang, X. Tang, Z. Wang *CrystEngComm.* **2011**, *13*, 1646–1653.
[39] G. J. Zhang, H. Li, F. F. Zhao, H. L. Hu, H. Huang, H. T. Li, X. Han, R. H. Liu, H. Dong, Y. Liu, Z. H. Kang *Dalton T.* **2013**, *42*, 9423–9427.
[40] R. Vaidhyanathan, D. Bradshaw, J. N. Rebilly, J. P. Barrio, J. A. Gould, N. G. Berry, M. J. Rosseinsky *Angew. Chem.* **2006**, *118*, 6645–6649.

Submitted: August 22, 2017
Revised: October 5, 2017
Accepted: October 9, 2017